PHYSICAL REVIEW B VOLUME 47, NUMBER 16 15 APRIL 1993-II

Center-of-mass quantization of excitons and polariton interference in GaAs thin layers

A. Tredicucci
Scuola Normale Superiore, I-56100 Pisa, Italy

Y. Chen
Scuola Normale Superiore, I-56100 Pisa, Italy
and Laboratoire de Microstructures et de Microélectronique (CNRS), 92220 Bagneux, France

F. Bassani
Scuola Normale Superiore, I-56100 Pisa, Italy

J. Massies, C. Deparis, and G. Neu
Laboratoire de Physique du Solide et Energie Solaire (CNRS), 06560 Valbonne, France
(Received 10 December 1992)

We report a detailed study of the properties of exciton polaritons confined in GaAs thin layers grown by molecular-beam epitaxy. Intermediate-layer thicknesses from 150 to 600 nm between quasi-two-dimensional quantum wells and bulk GaAs are considered. Both reflectance and photoluminescence measurements have been performed, and a large number of oscillation fringes and emission peaks have been detected. The spectra obtained are significantly different from those of a quantum well or of bulk GaAs, and can be attributed to quantized levels of the exciton-center-of-mass motion. The thickness dependence of the exciton peaks shows dominant contributions from the heavy-hole exciton dispersion due to its larger oscillator strength and density of states. Polariton effects and interference between different modes have to be taken into account to explain the reflectance behavior. This is done using three types of additional boundary conditions (ABC's). From the sensitive dependence of the reflectance line shape on different ABC's, we conclude that only Pekar's ABC gives interference fringes comparable to the experimental data. A temperature-dependence investigation gives clear evidence that the polariton effects manifest themselves in both optically thin and optically thick layers of GaAs only at low temperatures. At higher temperatures the optical transitions are more excitonlike. The results are discussed by modeling the exciton-broadening parameter as a function of the exciton-phonon interaction.

I. INTRODUCTION

For many years, the problem of exciton polaritons has attracted a lot of attention because it is fundamental for understanding light propagation in crystals.[1–5] Various techniques such as reflectance, transmittance, photoluminescence, and resonant Brillouin scattering and nonlinear techniques such as four-wave mixing and hyper Raman scattering have been used to detect polariton dispersion and its optical effects.[6–13] So far, most of these studies have been limited to the case of polaritons in the bulk.

In a geometry-confined system, polariton dynamics can be substantially different. For instance, in a quasi-two-dimensional quantum-well (QW) structure excitons are no more free in the growth direction and the polariton propagation is allowed only in the well plane. Because of carrier confinement, the exciton binding energy and oscillator strength are strongly enhanced. As a consequence, the dominant contribution near the transition edge is due to excitons.[14] Much less attention has been paid to the polariton propagation in QW planes.[15–18] In thin layers of intermediate thickness (typically several times the exciton radius), carrier confinement effects are absent but quantization of the exciton center-of-mass (c.m.) motion occurs.[19] Again, because of translational crystal symmetry breaking in the growth direction, exciton-polariton kinetics is highly anisotropic. Polariton wave packets can propagate in the layer plane but can only oscillate in the confinement direction. This gives rise to observable wave interference consequences. Many interesting features can be studied in thin layers which should be different from both QW and bulk crystal properties. A number of theoretical papers have been published on the subject of the exciton quantization and the polariton propagation in thin layers,[19–25] but only a few experimental works have been reported to date. In a GaAs film, Schultheis and coworkers[26] have observed by reflectance and transmittance measurements the effect of polariton quantization, but they found only three structures for a layer of thickness $L \simeq 500$ nm. Recently, Kusuno *et al.*[27] have studied the low-temperature photoluminescence spectra of several GaAs layers and observed a number of sharp emission peaks, which they attributed to the quantized levels of polariton dispersion in the bulk. However, because of thermodynamic distribution, only the lowest levels could be detected with two very thin layers, and their 520-nm-thick layer spectrum did not show any space quantization of the exciton motion. More recently, we have investigated the

 ©1993 The American Physical Society

reflectivity of high-quality molecular-beam-expitaxy-grown (MBE) GaAs and have obtained unambiguous evidence of polariton effects in relatively thick GaAs layers.[28] A larger number of polariton interference peaks have been observed in a 600-nm-thick layer, equally evident as those resolved in a free-standing thin film of II-VI semiconductors.[7] These have been preliminary interpreted as due to polariton interference with a three-branch dispersion curve. It is expected that with decreasing layer thickness the polariton interference effects would become less important and the exciton c.m. quantization should play a more direct role.

In this work we extend our investigation to the case of optically thin GaAs layers, i.e., $L < \lambda_{ph}$, where λ_{ph} is the photon wavelength in the crystal. The results obtained with different layer thickness (150 to 600 nm) will be analyzed and compared to the theory of exciton c.m. quantization and polariton interference. This paper is organized as follows. In Sec. II, we give experimental details for the sample growth condition and the measuring techniques. In Sec. III, we present a systematic analysis of the interference spectra obtained with samples of different thicknesses at different temperatures. The thickness dependence of the interference peaks will be compared to the exciton levels of the c.m. quantization, and the reflectance spectra will be analyzed in the framework of exciton susceptibility with a two-branch polariton dispersion. The exciton broadening and its temperature dependence will be studied in terms of surface roughening and of the exciton-phonon interaction. In Sec. IV we summarize the results of the present work.

II. EXPERIMENT

The samples used in the measurements were prepared using the molecular-beam-expitaxy (MBE) technique. They were grown at 600 °C on exactly oriented or slightly misoriented GaAs(001) substrates doped with $2-3\times10^{18}$ cm^{-3} Si. The GaAs layers with thicknesses ranging from 150 to 600 nm were embedded in either $Al_xGa_{1-x}As$ alloys or GaAs/AlAs short-period superlattices (SPS) with an average aluminum concentration of $\bar{x} \simeq 0.3$. The use of SPS has the purpose of achieving a better growth performance of the GaAs layers. Samples grown on *exactly oriented and slightly misoriented* substrates show qualitatively similar spectra. Only the reflectance line-shape details are different because of the difference in the interface. We will show the spectra obtained on samples that are grown differently and will concentrate on the main features which allow a simple theoretical analysis. Table I gives a list of the structure parameters of the samples for which data are presented.

The samples for the measurements were mounted in a He gas-flow cryostat which enables us to change the sample temperature from 4.2 K up to room temperature. A 100-W tungsten-wire lamp was used for reflectance experiments in a near-normal-incidence configuration. Photoluminescence (PL) was excited with a He-Ne laser or with a diode laser. The reflected or emitted light was dispersed with a double-grating monochromator with a spectral resolution of 0.04 Å and was detected by a cooled GaAs photomultiplier coupled with a lock-in amplifier. The spectra are then recorded with a digital data-acquisition system and a microcomputer.

III. EXPERIMENTAL RESULTS AND DISCUSSION

Figure 1 shows both photoluminescence and reflectance spectra of sample 882, obtained at 4.2 K. The PL structure is typical of the GaAs bulk, showing narrow emission bands due to free excitons at 1515.0 meV (E_x), to excitons bound to neutral donors (D^0X) at 1514.1 meV, to excitons bound to neutral acceptors (A^0X) at 1512.4 meV, and at 1511.1 meV, the so-called g line of Kunzel and Ploog.[29] For a GaAs layer of 600-nm thick-

TABLE I. Thickness and composition parameters of GaAs samples for which data are presented. All samples were grown by molecular-beam epitaxy on Si-doped GaAs substrates.

	882	883[a]	1016	1017	1079
Buffer layer	1.2 μm GaAs	1.2 μm GaAs	1.2 μm GaAs	1.3 μm GaAs	0.7 μm GaAs
				0.7 μm alloy[b]	0.69 μm alloy[b]
Bottom barrier	46 nm MQW[c]	46 nm MQW[c]	800 nm alloy[b]	100 nm SPS[d]	100 nm SPS[d]
Central GaAs layer	600 nm	600 nm	200 nm	200 nm	150 nm
Top barrier	820 nm SPS[d]	820 nm SPS[d]	100 nm alloy[b]	100 nm SPS[d]	100 nm SPS[d]
				14 nm alloy[b]	35 nm alloy[b]
Cap layer	4 nm GaAs	4 nm GaAs			3 nm GaAs

[a]Substrate slightly misoriented 4° toward GaAs(111) Ga plan.
[b]Alloy: $Al_{0.3}Ga_{0.7}As$ alloy.
[c]MQW: AlAs/GaAs multiple quantum wells ($\bar{x}=0.3$).
[d]SPS: AlAs/GaAs short-period superlattice ($\bar{x}=0.3$).

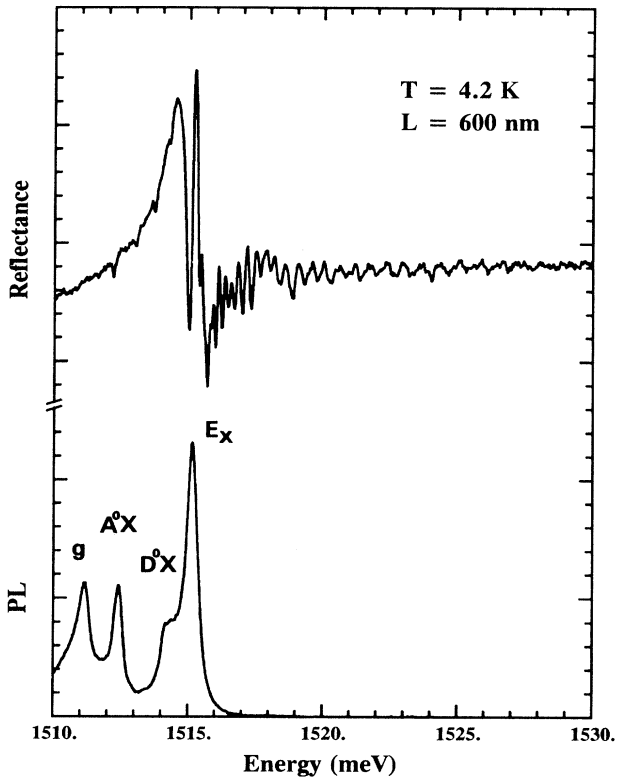

FIG. 1. Reflectance and photoluminescence spectrum of a MBE-grown GaAs thin layer (sample 882) with a nominal thickness of 600 nm, sandwiched between AlAs/GaAs superlattice barriers, measured at 4.2 K.

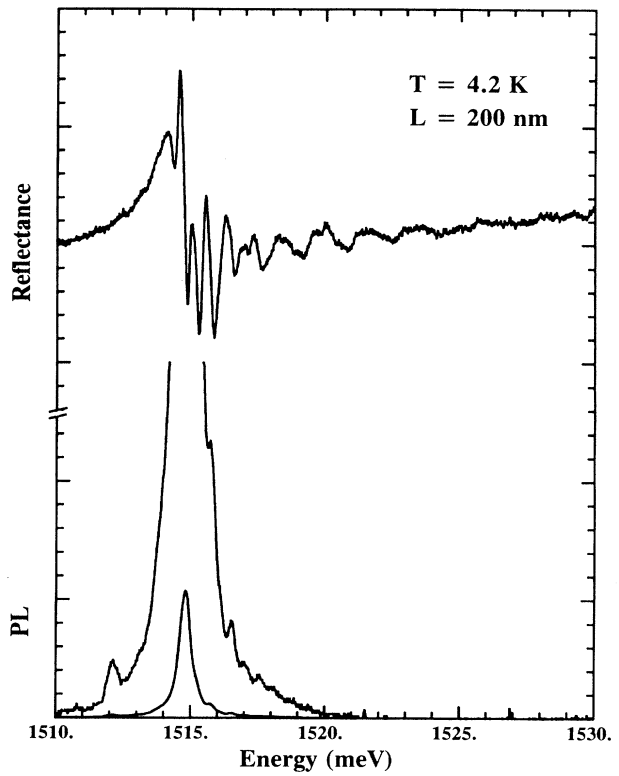

FIG. 2. Same as in Fig. 1 for sample 1016 with a nominal thickness of 200 nm.

ness we do not expect to detect emissions from quantized levels of the exciton states, because of the quasicontinuity of the exciton dispersion which allows efficient thermal relaxations.[27] In contrast, a larger number of oscillation fringes are well resolved in the reflectance spectrum, which can be analyzed in terms of polariton interference.[28]

Figure 2 shows a PL spectrum obtained with a diode laser excitation and a reflectance spectrum of sample 1017, with a GaAs layer thickness three times thinner than that of sample 882. They show, in addition to the reflection interference structure, a quantum structure in the emission peaks which will be proven as due to quantization of the exciton c.m. motion. We can notice that the positions of the peaks in the luminescence spectrum correspond to some of the minima in the reflectance spectrum, the strongest minima close to the exciton energy E_x having a corresponding luminescence peak.

Before going into a detailed analysis, we comment on several important features. First, the reflectance spectrum is clearly advantageous to the PL because it is more relevant to the density of states of all quantized levels. This allowed us to develop the following studies of the thickness and temperature dependences of the confined excitons or polaritons. Second, similar to the spectrum of a free-standing thin film of II-VI compound semiconductors, a large number of well-defined interference fringes is resoled in MBE samples. Since the MBE technique has advantages in the high quality of the thin layer preparation, many interesting features can be better studied. Third, due to valence-band degeneracy and the small value of the electron-hole exchange interaction, the interference in GaAs layers exhibits complicated structures near the exciton resonance energy. Although the interference structures well above E_x can be simply attributed to the exciton c.m. quantization, the structures near the $k=0$ exciton energy are due to superimposed multiple reflection and mutual interference. The polariton concept is necessary and a quantitative analysis will be developed in order to understand the exciton c.m. quantization and the polariton behavior.

A. Thickness dependence

Now we develop a more detailed analysis on the thickness dependence of the interference spectra of GaAs thin layers. Samples differently grown with equal nominal GaAs layer thickness (samples 882 and 883, 1016, and 1017) show similar interference features but somewhat different line shapes. For comparison we show in Figs. 3(a)–3(c) the spectra of sample 883 (600 nm), 1016 (200 nm), and 1079 (150 nm), measured at 4.2 K. Clearly, the interference structures strongly depend on layer thickness and the size effect increases with decreasing layer thick-

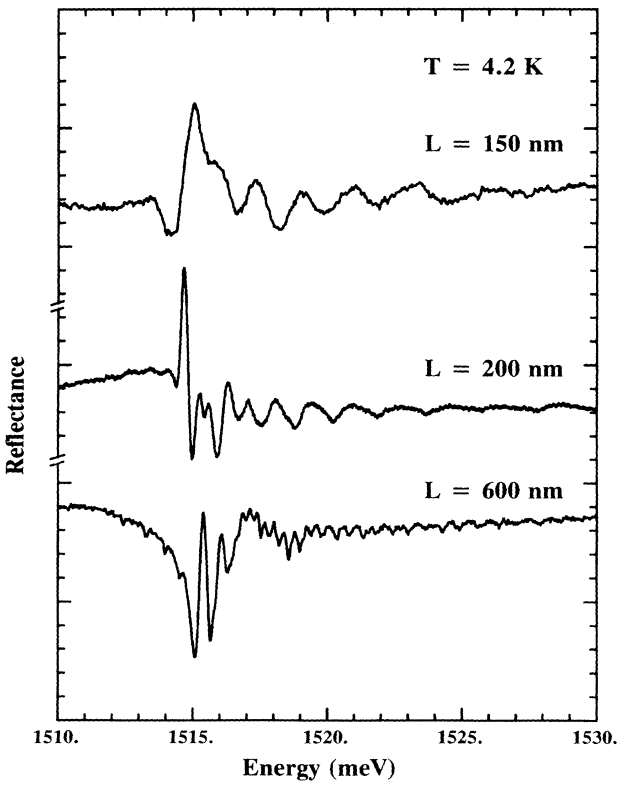

FIG. 3. Reflectance spectra of MBE-grown GaAs thin-layer structures, obtained at 4.2 K, with three layer thicknesses: 600 nm (sample 883), 200 nm (sample 1016), and 150 nm (sample 1079), in the spectral region of the exciton resonance.

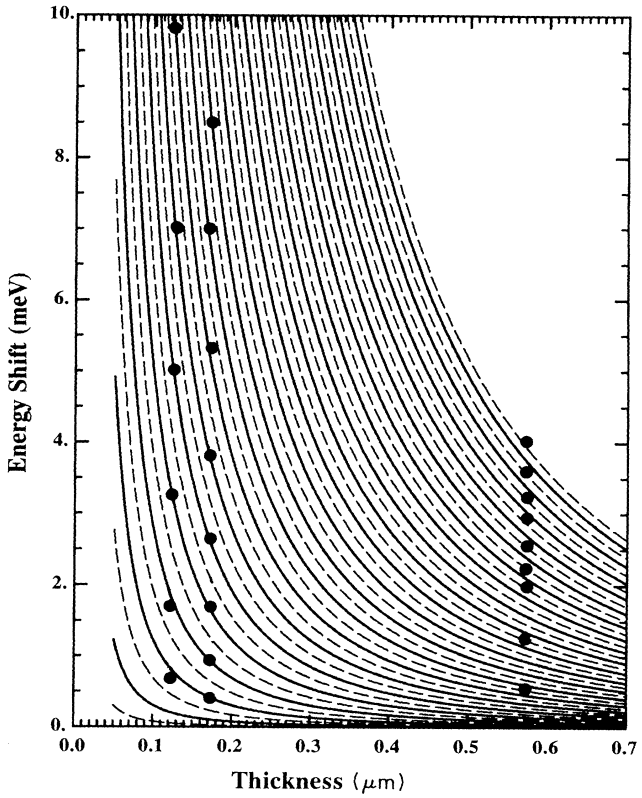

FIG. 4. Calculated center-of-mass quantization levels of heavy-hole exciton states confined in GaAs layers, with the effective mass $M_{ex}^{*}=0.49m_0$. The experimental data (points) are taken from the measured reflectance minima with the reduced effective layer thickness $L^{*}=L-2a_0^{*}$.

ness. We will first focus on the fast oscillations above the zero-momentum exciton energy.

Considering the exciton c.m. motion in the confinement direction with an effective layer thickness L^{*}, the quantum-mechanical boundary condition requires the exciton wave vector to be quantized as

$$k_n=n\frac{\pi}{L^{*}} \quad (n=1,2,3,\ldots) . \tag{1}$$

Neglecting the surface potential complexity and assuming a parabolic exciton band, the allowed states are given by

$$E_n=E_x+n^2\frac{\hbar^2\pi^2}{2M_{ex}^{*}L^{*2}} . \tag{2}$$

Such a simple picture immediately gives a reasonable account of the main features of our experimental results in the range of photon energy well above E_x. In Fig. 4, we plot the exciton energies versus the GaAs layer thickness, calculated using $M_{ex}^{*}=0.49m_0^{*}$, as the exciton effective mass and E_x as the energy origin. The solid (broken) lines are calculated for the even (odd) states. The experimental data (points) are taken from the reflectance minima of the experimental spectra (Fig. 3), assuming a reduced effective layer thickness $L^{*}=L-2a_0^{*}$, a_0^{*} being the exciton dead-layer thickness which will be discussed later. Apparently, the reflectance minima of the three spectra are in coincidence with the exciton quantized levels (2), and a parity selection rule clearly applies.

D'Andrea and Del Sole have given theoretical evidence of the exciton c.m. quantization by taking into account both the c.m. and the electron and hole relative motions.[19,20] In particular, they have introduced a variational parameter η to describe the exciton c.m. motion near the boundaries in the form of an evanescent wave $\exp(-\eta z)$. It turns out that the exciton quantized levels are given by two different equations for odd and even numbers with η as an input parameter. Variational calculations can be performed to find the value of η as a function of layer thickness. As expected, $1/\eta$ decreases with thickness for very thin layers. In the limit of not-too-thin layers the quantization can be approximated by (2), with a reduced effective thickness $L^{*}=L-2/\eta$ where $1/\eta$ has the same meaning as the exciton dead-layer thickness. It is then understood that such a dead layer is not a purely intrinsic parameter but is related to the structure geometry. To simplify, we do not try a variational approach for the best fit, but use the bulk exciton Bohr radius of GaAs as the exciton dead-layer thickness.

The exciton c.m. quantization energy (2) is sensitive to the value of the exciton effective mass. In our parabolic band approximation, the use of the heavy-hole exciton mass $M^*_{ex}=0.49m_0$ seems to be in overall agreement with the experimental data. As mentioned above, the exciton dispersion in the GaAs bulk is a two-branch curve: the *light- and heavy-exciton* bands. Kane and coworkers[30] have calculated the exciton-mass expression for small and large exciton wave vectors. In the case of small k, they obtained from a perturbative calculation two values of the exciton masses related to the off-diagonal matrix elements in the exciton Hamiltonian. Including the electron-hole exchange interaction, Fishman later worked out a three-branch polariton dispersion in GaAs.[31] Previously, we used this model to explain our reflectance data of the 600-nm-thick GaAs layer.[28] For much thinner layers, the exciton c.m. quantization plays an essential role and requires a reconsideration of exciton mixing. In fact, the c.m. quantization can now directly apply to the uncoupled *light- and heavy-hole excitons* and the mixing between the two can be neglected in first-order approximation. This is particularly true for the case of large exciton momentum where the off-diagonal correction can be neglected even in the bulk calculation. Assuming that the z axis is the quantization axis, the dispersion curve of the large momentum exciton is defined by

$$M^*_{ex}=m^*_{ez}+m^*_{hz} , \tag{3}$$

where

$$m^*_{hz}=m_0/(\gamma_1\mp 2\gamma_2) \tag{4}$$

are the effective masses of the *heavy* and *light holes,* respectively, γ_1 and γ_2 being Luttinger parameters. In GaAs $m_e^*=0.0665m_0$, $\gamma_1=6.85$, and $\gamma_2=2.1$; then $M^*_{ex}=0.44m_0$ (*heavy-hole exciton*) and $0.16m_0$ (*light-hole exciton*). Our experimental data show a reasonable agreement with expression (2) using simply the heavy-hole exciton mass. A reason for this preferential contribution could be the higher density of final states available and the larger values of the oscillator strengths in the heavy-hole exciton band.[8,30]

Concerning the parity selection rule, we refer to the model proposed by Kiselev *et al.*[32] and Merle and coworkers.[33,34] On the basis of the exciton c.m. quantization, these authors explicitly considered the exciton wave functions and the optical transition probabilities. They found that only the odd states are dipole active when $k_{ph}L^*=2\pi,4\pi,\ldots$, and only the even states are dipole active when $k_{ph}L^*=\pi,3\pi,\ldots$. In the case of $k_{ph}L^*=\pi/2,3\pi/2,\ldots$, both even and odd states are dipole active, having equal transition probabilities. In GaAs, $k_{ph}\approx 2.7\times 10^{-3}$ (Å^{-1}). Then it is expected that in 150- and 600-nm-thick layers the even states are likely to be dipole active, while in a 200-nm-thick layer both even and odd states are active, with comparable transition probabilities. Our experimental data show a clear parity selection but the reflectance minima do not correspond well to the quantum states of maximum transition probability. This can be understood by considering the multiple reflection in the top barrier. Closely depending on the sample geometry, an active state can give a peak or a dip in the spectral structure. Care has to be exercised in determining the transition parity from a reflectance spectrum.

Now we turn our attention to the polariton aspects of thin-layer optics. In relatively thick layers the polariton concept is clearly needed even for a qualitative explanation of the experimental features. As can be seen in the reflectance spectra of 600-nm-thick layers (Figs. 1 and 3), complicated interference structures appear near the $k=0$ exciton energy, which cannot be simply explained by the exciton c.m. quantization. In thinner layers, the polariton effect is expected to be less important, as shown by D'Andrea and Del Sole.[19] The oscillatory behavior of the 200- and 150-nm-thick layers seems to be easily explained with the c.m. quantization. However, the analysis of the singularity located at E_x and the parity selection rule on the quantized modes require the consideration of interference with the upper polariton mode.

To clarify the effect of interference between different modes on the reflectance spectra we show in Fig. 5 the dispersion of a polariton, as obtained from the eigenvalue equation

$$\frac{\hbar^2k^2c^2}{E^2}=\epsilon_b+\frac{4\pi\beta E^2_{ex}(k)}{E^2_{ex}(k)-E^2} , \tag{5}$$

where ϵ_b is the background dielectric constant, β is the exciton polarizability, and the exciton eigenvalue is $E_{ex}(k)=E_x+\hbar^2k^2/2M^*_{ex}$.

In the calculations we used the following values of the parameters: $M^*_{ex}=0.49m_0$, $E_x=1515$ meV, $\epsilon_b=12.56$,[8] $4\pi\beta=1.325\times 10^{-3}$,[31] and an exciton Bohr radius $a_0^*=136$ Å.[4]

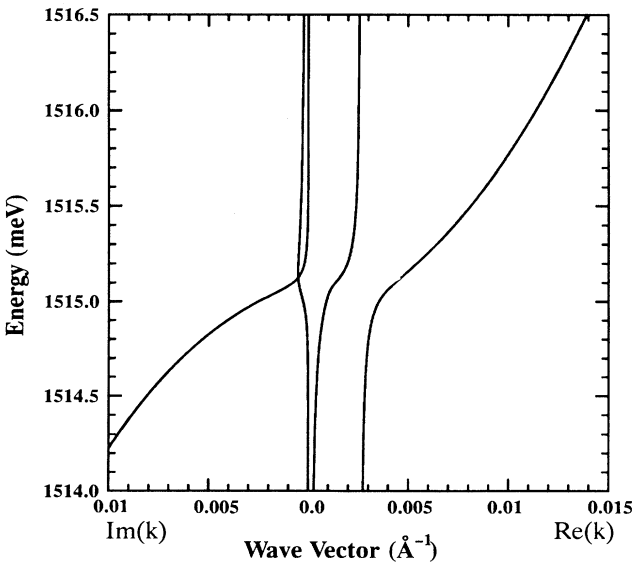

FIG. 5. Dispersion curve of the exciton polariton in bulk GaAs, calculated with the heavy-hole exciton parameters listed and with $\Gamma=0.1$ meV.

More complicated polariton dispersion can be obtained with degenerate and nonparabolic exciton bands.[31] Basically, the existence of at least two propagation modes in the crystal is essential for the manifestation of polariton effects.

Due to the presence of more than one propagation mode in the crystal, additional boundary conditions (ABC's) are needed to calculate the optical response of the system. The following ABC's have been proposed by Pekar (6a),[1] and by Birman and co-workers,[35,36] [Eqs. (6b) and (6c)]:

$$\text{ABC1: } \sum_i P_i|_{\text{surface}}=0 , \tag{6a}$$

$$\text{ABC2: } \sum_i \frac{\partial}{\partial z} P_i|_{\text{surface}}=0 , \tag{6b}$$

$$\text{ABC3: } \sum_i \left[\frac{\partial}{\partial z}+ik_+\right] P_i|_{\text{surface}}=0 , \tag{6c}$$

where P_i is the ith component of the excitonic contribution to the polarization and $k_+^2=(M_{\text{ex}}^*/\hbar^2 E_x)(E^2-E_x^2-i\Gamma E)$; others are given in the literature.[3] Of course, the need for ABC's is due to the use of a bulk dielectric function in Eq. (5). A nonlocal dielectric function computed from microscopic theory would automatically satisfy condition (6a) and give the intensity distribution ratio between the two or more polariton branches. With our model we need to choose one of the above ABC's to determine the relative intensities. In addition to the use of ABC's, an exciton free layer (dead layer) is included near each surface to take into account the surface potential and the finite size of the exciton. Then, if the exciton dead-layer thickness is D, the effective layer thickness will be reduced to $L^*=L-2D$. Typically, the exciton dead layer is of the order of the exciton Bohr radius, as shown by D'Andrea and Del Sole.[37] In the following we will use the exciton Bohr radius a_0^* as the dead-layer thickness, which is a good approximation for the case of $m_h^*/m_e^*\simeq 5$.[37]

With the above concepts we can perform a calculation of the reflectance in a multilayer sample as described in detail in the Appendix.

Figure 6 shows the results calculated with GaAs parameters and different ABC's for a 600-nm-thick layer system. The growth parameters are those listed in Table I for sample 882. Clearly, the spectra obtained with different ABC's show different behaviors both in their line shape near the $k=0$ exciton energy and in the intensity distribution over a large energy interval. Below E_x, ABC2 and ABC3 both give a well-defined dip structure while ABC1 gives a peak. Above E_x, the interference oscillations obtained with ABC1 extends over a few meV, in contrast to those obtained with ABC2 and ABC3. In addition, the Fabry-Perot–type interference of the upper polariton mode is clearly seen with (6a) and (6b) but not with (6c). We feel that the intensity distribution of the interference fringes provides information on the ABC dependence of the polariton dynamical response and the comparison with experimental results of Figs. 1, 2, and 3 justifies the validity of Pekar's condition (6a).

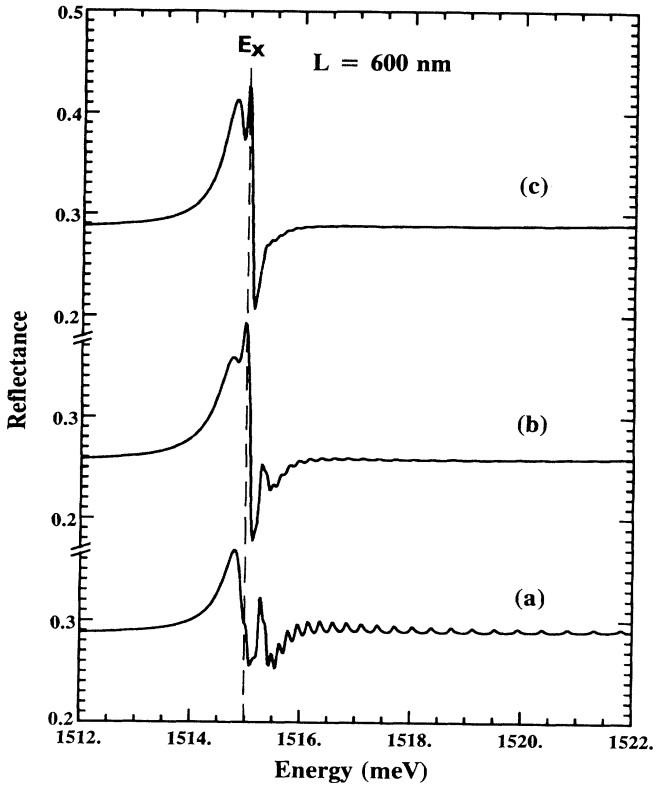

FIG. 6. Calculated reflectance spectrum of sample 882 with different ABC's: (a), (b), and (c) are given by Eq. (4). The parameters given in the text have been used. The vertical dashed line indicates the corresponding structures.

We have then computed the reflectance spectrum using ABC's (6a) with different layer thicknesses. The resulting reflectance minima and/or maxima are in a close coincidence with the exciton levels obtained by the c.m. quantization and contain the interference effects. Figure 7 shows one example of the calculated reflectance spectra, with the structure parameters of samples 1079 (Table I) and an exciton broadening $\Gamma=0.5$ meV. The two curves give a comparison of the spectra obtained using two different exciton effective-mass parameters: $M_{\text{ex}}^*=0.49m_0$ and $M_{\text{ex}}^*=\infty$, respectively. The spectral difference is striking, clearly demonstrating the effect of spatial dispersion in the polariton modes. In comparison with the experimental curve in Fig. 3 for $L=150$ nm, we can conclude that the polariton manifestation is undoubtable, and a reasonable agreement in the line shape requires a broadening parameter as large as $\Gamma=0.5$ meV. Different values of the broadening parameter are required for different layer thicknesses; in comparison with our experimental spectra we obtain the fitting values of $\Gamma_0=0.1$, 0.3, and 0.5 meV for the layer thickness of 600, 200, and 150 nm, respectively. The fact that the exciton broadening increases with decreasing layer thickness can be understood in the Hopfield model as an effect of the increased surface-to-bulk ratio.[38] In addition, a nonideal growth condition can result in growth steps at the inter-

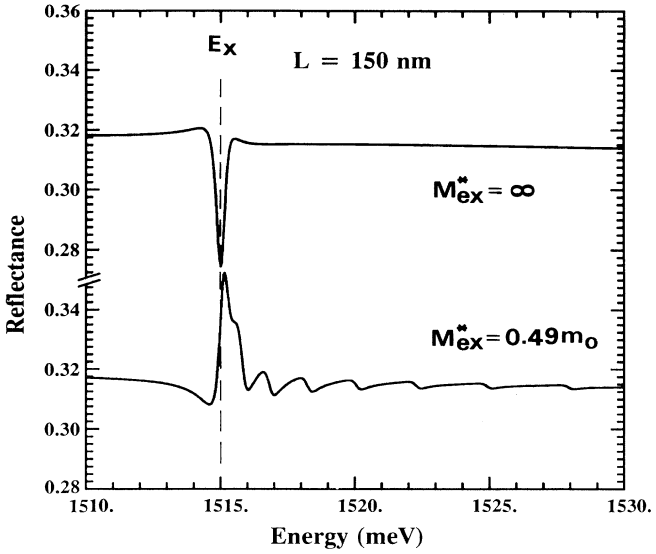

FIG. 7. Calculated reflectance spectrum of a 150-nm-thick GaAs layer with the exciton effective mass $M^*_{ex}=0.49m_0$ and $M^*_{ex}=\infty$. The parameters used are those listed and the broadening parameter is $\Gamma=0.5$ meV.

face and thickness fluctuations which give rise to an enhanced inhomogeneous broadening in thinner layers.

B. Temperature dependence

Reflectance spectra have also been studied as a function of temperature in order to obtain additional information. The results obtained with a 600-nm-thick GaAs layer (sample 882) are presented in Fig. 8. We observe that, as the temperature is raised, the structure shifts slightly to lower energy due to the variation of the band gap. Similarly, the fast oscillation structures, except the lowest three peaks, labeled *A*, *B*, and *C*, strongly reduce their oscillation amplitudes. The behavior of the *A*, *B*, and *C* peaks is more interesting. At lower temperature, peak *A* is dominant and its amplitude decreases with increasing temperature. Above 30 K, it disappears completely. In contrast, dip *B* is weak at low temperature and becomes dominant at higher temperatures. Peak *C* shows a smooth decrease of its amplitude with increasing temperature. The Fabry-Perot envelope structure looks the same over the temperature range because of its photonlike characteristics.

To explain the temperature behavior of our data, we first consider the general expression for exciton broadening,

$$\Gamma(T)=\Gamma_0+\sigma T+\gamma N_{\mathrm{LO}}(T)\ , \tag{7}$$

where the last two terms arise from the interaction with acoustic phonons and LO phonons, and the Bose function for the LO-phonon occupation is

$$N_{\mathrm{LO}}(\omega_0)=\frac{1}{\exp(\hbar\omega_0/kT)-1}\ . \tag{8}$$

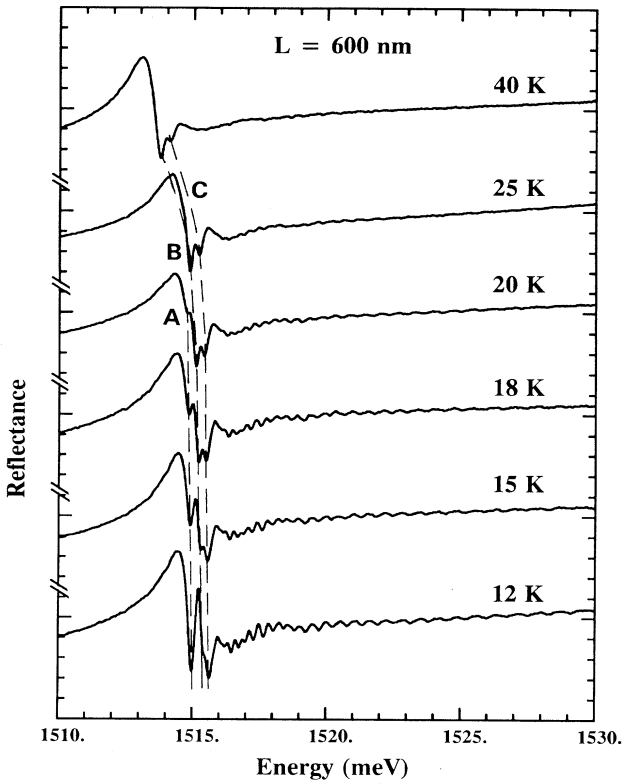

FIG. 8. Reflectance spectra of a 600-nm-thick GaAs layer (sample 882), measured at various temperatures. Vertical lines are inserted to indicate the corresponding structures.

In the temperature range of interest, the exciton broadening depends linearly on the temperature T and the main contribution comes from the exciton-acoustic-phonon interaction. We have calculated the reflectance spectra as a function of $\Gamma(T)$ and then compared them with those obtained experimentally at various temperatures. From the amplitude decrease of the oscillation fringes, we have estimated the Γ value as a function of temperature and obtain the linear coefficient $\sigma\approx 14$ μeV/K. This value is consistent with the previous finding of Schultheis *et al.*[39] who used four-wave mixing and the transmittance technique on their 100–190-nm-thick samples ($\sigma\approx 17$ μeV/K).

We can also verify that the polariton effect is important only in the case where the exciton broadening parameter Γ is less than the critical value

$$\Gamma_c=\left[\frac{8E_{\mathrm{LT}}E_x^2\epsilon_b}{M^*_{ex}c^2}\right]^{1/2}\ , \tag{9}$$

where E_{LT} is the exciton transverse-longitudinal splitting, given by $E_{\mathrm{LT}}=(2\pi\beta/\epsilon_b)E_x$, as shown by Tait.[40] Using the GaAs parameters listed, we obtain $\Gamma_c=0.27$ meV. At the higher temperatures where $\Gamma>\Gamma_c$, the exciton-phonon coupling becomes dominant and the polariton features are washed out as if excitons and photons were independent modes. This seems to be a possible explana-

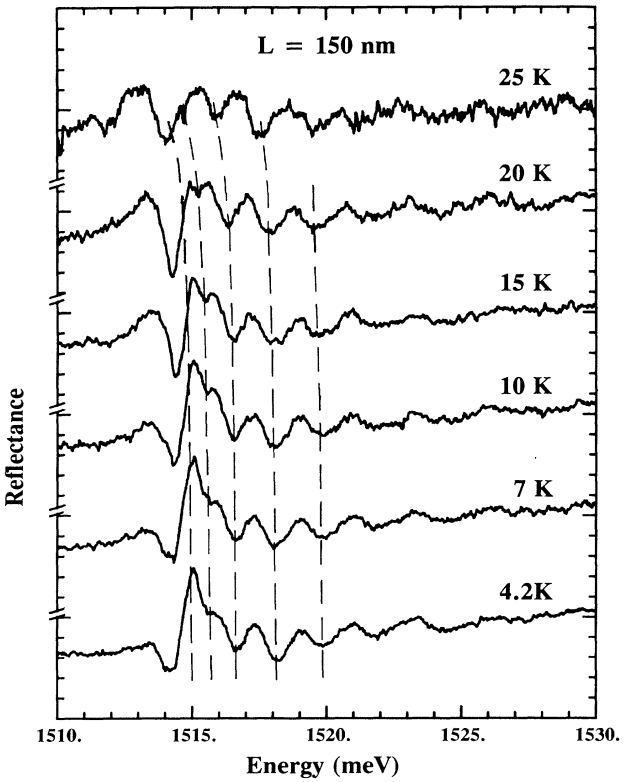

FIG. 9. Same as in Fig. 8 for sample 1079 with a nominal thickness of 150 nm.

tion for the observed behavior of the A and B peaks. We assign peak A to a polariton feature and peak B to an excitonic transition. The relative change of the A and B peak strength suggests a possible coexistence of the two excitation types. That is, at intermediate temperature range, only a fraction of the optically excited excitons are coherently coupled with the electromagnetic field of incident light while a fraction of the excitons is subject to a normal absorption process by the perturbing radiation.

This model is further confirmed by the temperature dependence of the reflectance spectrum of the 150-nm sample 1079, shown in Fig. 9. Again, all the structure above E_x shifts slightly to lower energy as the temperature increases but the lowest structure does not follow this rule. Apparently, the structure at 1515 meV changes from peaklike to diplike as shown in the theoretical calculation of Fig. 7 where the calculated polariton reflectance ($M_{ex}^{*}=0.49m_0$) shows a peaklike structure while the exciton reflectance ($M_{ex}^{*}=\infty$) gives a diplike structure. Our data on sample 1079 indicate that the spectral nature changes from polaritonlike to excitonlike at a temperature of 15–20 K, which is consistent with our interpretation of the temperature behavior of sample 882.

IV. CONCLUSIONS

By comparing reflectance and luminescence data with the polariton model theory we have shown both c.m. quantization of the excitonlike mode and interference between the photon mode and the additional ray. We note that the exciton c.m. quantization also gives a good prediction on the interference peak position for thin and thick layers, but the identification of the transition parity requires a more detailed calculation of the reflectance which includes polariton effects. In that case, the calculation based on the exciton-polariton susceptibility implicitly includes exciton c.m. quantization,[20,22,32] and it also accounts for the Fabry-Perot interference.

In conclusion, we have studied the reflectance and photoluminescence spectra of GaAs thin layers. The reflectance structure and the emission peaks have been interpreted as evidence for the exciton center-of-mass quantization and the interference between polariton modes. From the line-shape analysis, we conclude that the polariton effect can be observed in GaAs films of different layer thickness but it is washed out at high temperature.

ACKNOWLEDGMENTS

This work was supported by the European Community through Contract No. ST2J-0254, and by the Italian C.N.R. (National Research Council). One of us (Y.C.) is very indebted to the Scuola Normale Superiore di Pisa for kind hospitality.

APPENDIX: CALCULATION ALGORITHM FOR THE REFLECTANCE SPECTRUM IN THIN LAYERS

In this appendix we give an algorithm for the calculation of the reflectance including polariton effects with spatial dispersion. Considering the polariton wave vector k_i ($i=1,2$) in the direction perpendicular to the layer planes, the electric and magnetic fields inside the layer can be expressed as

$$E(z)=\sum_{j=1}^{2}(E_j^{+}e^{ik_jz}+E_j^{-}e^{-ik_jz}) , \tag{A1}$$

$$B(z)=\sum_{j=1}^{2}\frac{\omega}{c}k_j(E_j^{+}e^{ik_jz}-E_j^{-}e^{-ik_jz}) , \tag{A2}$$

where $E_1^{\pm}$ and $E_2^{\pm}$ are four complex field amplitudes which characterize two forward and two backward propagations. If the layer thickness is l_a, the transfer matrix m_a is defined by

$$\begin{bmatrix} E\left[\frac{-l_a}{2}\right] \\ B\left[\frac{-l_a}{2}\right] \end{bmatrix} = m_a \begin{bmatrix} E\left[\frac{l_a}{2}\right] \\ B\left[\frac{l_a}{2}\right] \end{bmatrix} . \tag{A3}$$

The additional boundary conditions are needed to determine m_a. We consider the exciton polarization field,

$$P(z)=\sum_{j=1}^{2}\epsilon_j(E_j^{+}e^{ik_jz}+E_j^{-}e^{-ik_jz}) \tag{A4}$$

with

$$\epsilon_j=\frac{c^2}{\omega^2}k_j^2-\epsilon_b \quad (j=1,2)\ . \tag{A5}$$

By applying an ABC at the left ($z=-l_a/2$) and the right ($z=+l_a/2$) surfaces, we obtain two additional equations. This allows us to set a relation between the four variables, for instance,

$$\begin{bmatrix}E_2^{+}\\E_2^{-}\end{bmatrix}=Q_\tau\begin{bmatrix}E_1^{+}\\E_1^{-}\end{bmatrix}, \tag{A6}$$

with

$$\text{ABC1:}\quad Q_1=-\frac{\epsilon_1}{\epsilon_2}\begin{bmatrix}\lambda_2^{*} & \lambda_2\\ \lambda_2 & \lambda_2^{*}\end{bmatrix}^{-1}\begin{bmatrix}\lambda_1^{*} & \lambda_1\\ \lambda_1 & \lambda_1^{*}\end{bmatrix}, \tag{A7}$$

$$\text{ABC2:}\quad Q_2=-\frac{k_1\epsilon_1}{k_2\epsilon_2}\begin{bmatrix}\lambda_2^{*} & -\lambda_2\\ \lambda_2 & -\lambda_2^{*}\end{bmatrix}^{-1}\begin{bmatrix}\lambda_1^{*} & -\lambda_1\\ \lambda_1 & -\lambda_1^{*}\end{bmatrix}, \tag{A8}$$

$$\text{ABC3:}\quad Q_3=-\frac{\epsilon_1}{\epsilon_2}\begin{bmatrix}(k_++k_2)\lambda_2^{*} & (k_+-k_2)\lambda_2\\ (k_++k_2)\lambda_2 & (k_+-k_2)\lambda_2^{*}\end{bmatrix}^{-1}\times\begin{bmatrix}(k_++k_1)\lambda_1^{*} & (k_+-k_1)\lambda_1\\ (k_++k_1)\lambda_1 & (k_+-k_1)\lambda_1^{*}\end{bmatrix}, \tag{A9}$$

and

$$\lambda_j=\exp\left[ik_j\frac{l_a}{2}\right]. \tag{A10}$$

Now, eliminating the amplitude variables by the values of the electric and magnetic fields at the two boundaries, the transfer matrix results in

$$m_a=\left[\begin{bmatrix}\lambda_1^{*} & \lambda_1\\ n_1\lambda_1^{*} & -n_1\lambda_1\end{bmatrix}+\begin{bmatrix}\lambda_2^{*} & \lambda_2\\ n_2\lambda_2^{*} & -n_2\lambda_2\end{bmatrix}Q_\tau\right]\times\left[\begin{bmatrix}\lambda_1 & \lambda_1^{*}\\ n_1\lambda_1 & -n_1\lambda_1^{*}\end{bmatrix}+\begin{bmatrix}\lambda_2 & \lambda_2^{*}\\ n_2\lambda_2 & -n_2\lambda_2^{*}\end{bmatrix}Q_\tau\right]^{-1}, \tag{A11}$$

where the Q_τ matrix is different for the three ABC's.

When the frequency is sufficiently far from the resonance frequency of the medium, which is the case for reflections between different barriers, the transfer matrix reduces to the usual form,[41]

$$m_j=\begin{bmatrix}\cos\left[\frac{\omega}{c}n_al_a\right] & -i\frac{1}{n_a}\sin\left[\frac{\omega}{c}n_al_a\right]\\ -in_a\sin\left[\frac{\omega}{c}n_al_a\right] & \cos\left[\frac{\omega}{c}n_al_a\right]\end{bmatrix}. \tag{A12}$$

Knowing the transfer matrix of each layer, the matrix product

$$M=m_1m_2\cdots m_j\cdots m_N \tag{A13}$$

gives the transfer matrix of the total system containing N layers. In our MBE-grown samples, the multiple layers were grown on thick substrates in which the incoming radiation is in the region of interband transitions (above exciton ionization). In this case, the reflectance at the interface is simply given by Fresnel relations, so that the total reflectivity becomes

$$r=\frac{1-n_{\text{eff}}}{1+n_{\text{eff}}}, \tag{A14}$$

with

$$n_{\text{eff}}=\frac{M_{11}+n_{\text{sub}}M_{12}}{M_{21}+n_{\text{sub}}M_{22}}, \tag{A15}$$

and M_{ij} are the four matrix elements of M.

[1]S. I. Pekar, Zh. Eksp. Teor. Fiz. **33**, 1022 (1957) [Sov. Phys. JETP **6**, 785 (1958)], see also *Crystal Optics and Additional Light Waves* (Benjamin-Cummings, Menlo Park, CA, 1983).

[2]H. Hopfield, Phys. Rev. **112**, 155 (1958); H. Hopfield and D. G. Thomas, *ibid.* **132**, 563 (1963).

[3]See, for instance, J. L. Birman, L. Koteles, and E. L. Ivchenko, in *Excitons, Modern Problems in Condensed Matter Sciences* (North-Holland, Amsterdam, 1982), Vol. 2.

[4]C. Weisbuch and R. G. Ulbrich, in *Light Scattering in Solids III,* edited by M. Cardona and G. Günterodt, Springer Topics in Applied Physics Vol. 51 (Springer-Verlag, Berlin, 1982), p. 207.

[5]F. Bassani and L. C. Andreani, in *Excited State Spectroscopy in Solids,* Proc. S.I.F., Course XCVI, edited by N. Terzi (North-Holland, Amsterdam, 1987), p. 1.

[6]D. D. Sell, S. E. Stokowski, R. Dingle, and J. V. Dilorenzo, Phys. Rev. B 7, 4569 (1972).

[7]V. A. Kiselev, B. S. Razbirin, and I. N. Uraltsev, Phys. Status Solidi B **72**, 161 (1975).

[8]R. G. Ulbrich and C. Weisbuch, Phys. Rev. Lett. **38**, 865 (1977).

[9]B. Hönerlage, A. Bivas, and Vu Duy Phach, Phys. Rev. Lett. **41**, 49 (178).

[10]T. Mita and N. Nagasawa, Solid State Commun. **44**, 1003 (1982).

[11]M. Matsuskita, J. Wickstel, and H. Z. Cammius, Phys. Rev. B **29**, 3362 (1984); J. Wickstel, M. Matsuskita, H. Z. Cammius, T. Shigenar, and X. Z. Lu, *ibid.* **29**, 3350 (1984).

[12]Y. Chen, B. Gil, and H. Mathieu, Ann. Phys. (Paris) **12**, 109 (1987).

[13]D. Fröhlich, A. Kulik, B. Uebbing, A. Mysyrowicz, V. Langer, H. Stotz, and W. von des Osten, Phys. Rev. Lett. **67**, 2343 (1991).

[14]See, for example, *Physics and Application of Quantum Wells and Superlattices,* Vol. 170 of *NATO Advanced Study Institute, Series B: Physics,* edited by E. E. Mendez and K. Van

Klitzing (Plenum, New York, 1987).
[15]M. Nakayama, Solid State Commun. **55**, 1053 (1985).
[16]L. C. Andreani and F. Bassani, Phys. Rev. B **41**, 7536 (1990).
[17]F. Tassone, F. Bassani, and L. C. Andreani, Nuovo Cimento D **12**, 1673 (1990); Phys. Rev. B **45**, 6023 (1992).
[18]K. Ogawa, T. Katsuyama, and H. Nakamura, Phys. Rev. Lett. **64**, 796 (1990).
[19]A. D'Andrea and R. Del Sole, in *Excitons in Confined Systems,* edited by A. D'Andrea, R. Del Sole, and A. Lapiccirella, Proceedings in Applied Physics Vol. 25 (Springer-Verlag, Berlin, 1988), p. 128.
[20]A. D'Andrea and R. Del Sole, Phys. Rev. B **41**, 1431 (1990).
[21]H. Ishihara and K. Cho, Phys. Rev. B **41**, 1424 (1990).
[22]K. Cho and H. Ishihara, in *Excitons in Confined Systems* (Ref. 19), p. 90; K. Cho, A. D'Andrea, R. Del Sole, and H. Ishihara, J. Phys. Soc. Jpn. **59**, 1853 (1990).
[23]G. Czajkowski and P. Schillak, Nuovo Cimento D **11**, 1535 (1989).
[24]G. Czajkowski and A. Tredicucci, Nuovo Cimento D **14**, 1203 (1992).
[25]F. Bassani, G. Czajkowski, A. Tredicucci, and P. Schillak, Nuovo Cimento D (to be published).
[26]L. Schultheis and K. Ploog, Phys. Rev. B **29**, 7058 (1984); L. Schultheis, K. Köhler, and C. W. Tu, in *Excitons in Confined Systems* (Ref. 19), p. 110.
[27]J. Kusuno, Y. Segawa, M. Mihara, Y. Aoyagi, and S. Namba, Solid State Commun. **72**, 218 (1989).
[28]Y. Chen, F. Bassani, J. Massies, C. Deparis, and G. Neu, Europhys. Lett. **14**, 483 (1991).
[29]H. Kunzel and K. Ploog, in Proceedings of the 8th International Symposium on GaAs and Related Compounds, IOP Conf. Proc. No. 56 (Institute of Physics and Physical Society, London, 1981), p. 519.
[30]E. O. Kane, Phys. Rev. B **11**, 3850 (1975); M. Altarelli and N. O. Lipari, *ibid.* **15**, 4898 (1977).
[31]G. Fishman, Solid State Commun. **27**, 1097 (1977).
[32]V. A. Kiselev, I. V. Makarenko, B. S. Razbirin, and I. N. Uraltsev, Fiz. Tverd. Tela (Leningrad) **19**, 2348 (1977) [Sov. Phys. Solid State **19**, 1374 (1977)].
[33]Y. Merle d'Aubigné, Le Si Dang, A. Wasiela, N. Magnea, F. Dal'Bo, and A. Million, J. Phys. (Paris) **48**, C5363 (1985).
[34]H. Tuffigo, R. T. Cox, N. Magnea, Y. Merle d'Aubigné, and A. Millon, Phys. Rev. B **37**, 4310 (1988).
[35]J. L. Birman and J. J. Sein, Phys. Rev. B **6**, 2482 (1975).
[36]C. S. Ting, M. J. Franckel, and J. L. Birman, Solid State Commun. **17**, 1285 (1975).
[37]A. D'Andrea and R. Del Sole, Phys. Rev. B **32**, 2337 (1985).
[38]J. J. Hopfield, J. Phys. Soc. Jpn. **21**, 77 (1966).
[39]L. Schultheis, R. J. Kuhl, A. Honold, and C. W. Tu, Phys. Rev. B **34**, 9027 (1986); in *Excitons in Confined Systems* (Ref. 19), p. 50.
[40]W. C. Tait, Phys. Rev. B **5**, 648 (1972).
[41]M. Born and F. Wolf, *Principles of Optics* (Pergamon, Oxford, 1980).